Journal of High School Science

Electrospun poly(styrene-b-isoprene-b-styrene)/C5 pressure-sensitive adhesives with cross-linked structures

Mucheng Ma[1], Ruth Wahl

ABSTRACT

Poly(styrene-b-isoprene-b-styrene) (SIS) solution was directly electrospun into nonwoven cross-linked membranes under various processing conditions. An optimized condition was adopted to electrospin SIS/C5 pressure-sensitive adhesives (PSAs) with spider web similar structures. The morphology and adhesive properties of SIS/C5 PSAs were measured at different electrospinning conditions such as solution concentration, SIS/C5 ratio, voltage and tip-to-collector distance. The results indicated that the morphology and adhesive properties of the fibers could be altered depending on the electrospinning conditions. Increasing the C5 resin content from 30 to 70 wt%, increased the 180° peeling strength 15 times (from 0.03 to 0.45 kN/m) while simultaneously decreasing the porosity and water vapor penetration rate (1.4 % and 0.9 g/cm^2×h). The diameter of the SIS/C5 fibers increased with the increment of C5 content, leading to the disappearance of pore structures. The adhesive properties and morphology of the fibers followed a similar trend as their thickness increased. Thus, an optimum SIS/C5 ratio (50:50) and membrane thickness (50 μm) were required for acceptable adhesive performance and cross-linked morphology along with acceptable porosity, water vapor penetration rate and mechanical stability.

Key words: pressure-sensitive adhesives; electrospun nanofibers; thermoplastic elastomer; adhesive performance

---

1. Corresponding author, New Hampton School, 70 Mainstreet, New Hampton, NH, USA 03256, Tel: +86-188-4129-7517 E-Mail: 3313617810@qq.com

1. Introduction

Spider silk is ubiquitous in nature and possesses unique performances such as strong mechanical strength, large specific surface area and good adhesion in order to capture insects (spider silk protein (spidroin) adhesive). However, spiders are difficult to breed. It is challenging to obtain spider silk on a large scale by artificial breeding. To imitate spider silk, many polymers have been widely investigated as electrospun fibers with average diameters in the range from nanometers to micrometers. The properties of these electrospun fibers have been extensively explored in many fields such as microfiltration, biomedical and tissue engineering, transdermal patches, and medical adhesive tape (1,2).

Many polymeric materials can be electrospun into non-woven membranes. These membranes are different from spider webs in that (a) they are formed by physical stacking without cross-linked structures; (b) most of them have no macroscopic cohesiveness. In the former case, non-woven membranes lacked sufficient strength due to weak connections among adjacent fibers. To resolve this issue, researchers introduced cross-linked structures among adjacent fibers by a heating treatment (3) or using chemical methods (4). However, the post-treatments typically led to membrane shrinkage, fiber thickening, or reduced porosity (5). In the latter case, the lack of adhesion limited their applications in some cases. For example, they could not be directly used in the field of transdermal patches and had to tightly contact the skin surfaces with the aid of external assistance, such as suturing (6) or the interjection of an adhesive layer (7).

Pressure-sensitive adhesives (PSAs) are a class of adhesive materials that are permanently tacky without recourse to solvent evaporation or chemical reaction at room temperature. They can immediately adhere to any substrate at low pressure, and be easily removed without leaving residues on the adhering substrate surfaces (8). Among various PSAs, poly(styrene-b-isoprene-b-styrene) (SIS) based pressure-sensitive adhesives are widely used due to their simple composition, convenience and environmentally friendly features (9). They mainly consist of SIS, a tackifier (such as C5 aliphatic hydrogenated resin), mine oil and an antioxidant, in which the mine oil adjusts the melting processing temperature by acting as a plasticizer. They are usually processed by hot-melt coating or solution coating. However, their air permeability is low, which restricts their applications (10). In this study, SIS based PSAs were formulated without a plasticizer by the electrospinning technology. These non-woven PSAs were similar in structure and properties to spider webs because (a) they had adhesive performance due to the basic composition of PSAs; (b) SIS could strongly strengthen the electrospun PSAs due to the favorable orientation of their chains during the electrospinning process; (c) the adjacent fibers could form networks via cross-linking. Their structures and properties could be optimized by varying their processing conditions such as electrospinning voltage, solution concentration and the SIS/C5 ratio.

2. Experimental section

2.1. Materials

SIS polymer (YH-1105, Mn～$8x10^4$ Da, diblock ＜ 1%, styrene 15 wt%) was supplied by Sinopec Baling Petroleum & Chemical Co., China. C5 resin (C-100R, Eastman Chemical Company, USA) was used as a tackifier. Tetrahydrofuran (THF), N,N-Dimethylformamide (DMF), and cyclohexane (CYH) were purchased from Tianjin Kemio Fine Chemical Co, China. All chemicals were used as received.

2.2. Fabrication of nonwoven PSAs

A mixture of DMF, THF and CYH at a weight ratio of 50/25/25 was used to electrospin SIS solution with a concentration of 10 to 16 wt% between voltages of 10 to 25 kV at 25±2°C. The solution was loaded into four 10 mL plastic syringes fixed on the slipway of the electrospinning equipment (Changsha Nano instrument Co, Ltd, China) and injected through 23-G metal needles with a controllable feed rate of 1 mL/h. The fibers were deposited on a rotating drum collector covered with hydrophilic polycarbonate filter film (ϕ=0.4 μm). A factorial experiment was designed to investigate the relative significance of solution concentration and electrospinning voltage on the structures of nonwoven membranes. To ensure the uniformity of nonwoven membranes, the four plastic syringes were placed on an injection pump, and the pump horizontally moved backward and forward at a speed of 200 cm/min within a fixed distance using the mechanical slide unit. Furthermore, electric shield devices on the needles were also employed to ensure that the jets were only generated in the forward direction; thus, the resultant fibers could be uniformly deposited during the quadrature motion process caused by the synchronous movement of the rotating drum collector and mechanical slide unit. The collector speed was 400 RPM, and the tip-to-collector distance was 15 to 25 cm. The ambient temperature was 25±2 °C, and the relative humidity was 40 %. Fabricated samples were vacuum-dried at 40 °C for 1 h to remove the residual solvent and static charge. These optimized electrospinning conditions were used to fabricate SIS/C5 nonwoven membranes. The various SIS/C5 weight ratios used were 7:3, 6:4, 5:5, 4:6 and 3:7. The solution concentration increased from 16 to 24 wt % with the increase of C5 weight ratio. The thickness of nonwoven membranes could be controlled by varying the deposition time.

2.3. Measurements of structure and properties

The morphology of nonwoven membranes was examined by scanning electron microscopy (SEM; QUANTA 450, FEI Ltd., USA). Prior to examination, the samples were gold sputtered in a vacuum evaporator (JEE-4X, Japan). The thickness of each membrane was measured by a high-precision thickness gauge (CHY-C2, Labthink Co., Ltd, China). The water vapor penetration rate (*WVP*) was measured with a moisture permeable cup, according to the assembly shown in Figure 1.

Figure 1 Schematic setup for *WPR* measurement.

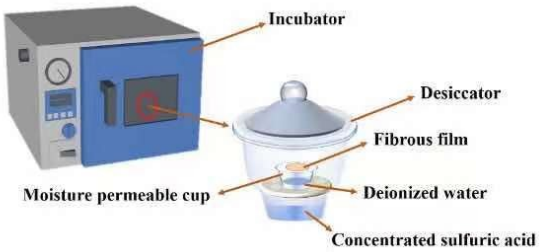

First, the moisture permeable cup (diameter, 60mm) was filled with an appropriate amount of de-ionized water and sealed with the nonwoven membrane. Its mass (m_0), was measured. The cup was placed in the desiccator with concentrated

sulfuric acid as shown in the figure. The desiccator was kept in a constant temperature oven (23±2 °C). The mass of the cup (m) was measured at 6 hour intervals for a total time of 72 hours. The mass of the cup was plotted as a function of the time t and resulted in a straight line according to equation 1.

$$m = m_o - (WVP * S * t) \quad \text{Equation 1}$$

Where S is the measured area of the nonwoven membrane (cm^2); t is the test time (h); m_0 and m (g) are the initial mass and the mass measured at time t, respectively. This is a linear function with t as independent variable and m as dependent variable. WVP can be calculated from the slope ($WVP * S$) of the m versus t curves.

The porosity was measured by n-butanol immersion method with a blank polycarbonate filter and nonwoven membranes (2cm×2cm). They were immersed in n-butanol for 12 hrs at room temperature. Their porosity was calculated according to equation (2).

$$P(\%) = \frac{(M_1 - M_0) - (m_1 - m_0)}{4\rho * (H_0 - h_0)} \quad \text{Equation 2}$$

Where M_0 and M_1 are the mass of nonwoven membrane before and after immersion; m_0 and m_1 are the mass of blank polycarbonate filter before and after immersion; and H_0 and h_0 are the thickness of nonwoven membrane and blank polycarbonate filter, respectively; ρ is the density of n-butanol (g/cm^3).

The 180º peel strength and holding power of nonwoven membranes were measured using a BLD-S electronic all-powerful stripping machine (Labthink Instruments Co., Ltd., China) at a peeling rate of 300 mm/min. The samples were cut into strips with 25mm x 100mm dimensions and these strips were pressed onto clean stainless-steel substrates with a 2 kg rubber roller at room temperature and then left to stand for over 20 min to obtain sufficient adhesion. The average value of 180º peel strength for the samples was determined from a minimum of three specimens. The holding power of nonwoven membranes was measured with a CZY-6 holding adhesive testing instrument (Labthink Instruments Co., Ltd., China). Specimen strips with 25mm x 70mm dimensions were pressed onto clean stainless-steel substrates with a 2kg rubber roller. The roller was moved backward and forward three times. The specimens were left to stand for over 20 min at 25±2 °C prior to characterization. Tests were performed on three specimens to allow calculation of an average value.

3. Results and discussion

3.1. Optimization of electrospinning conditions

In this study, the SIS functioned as the skeleton of nonwoven SIS/C5 PSAs. Thus, it became an important prerequisite of successfully fabricating nonwoven SIS/ C5 PSAs to control the structure and morphology of electrospun SIS membranes by optimizing various electrospinning conditions, such as solution concentration, voltage and thetip-to-collector distance. We investigated the influence of solution concentration on the morphology of SIS membranes, which were electrospun with different concentrations (10 wt%, 13 wt% and 16 wt%) using an electrospinning voltage of 20 kV and a tip-to-collector distance of 20 cm. As shown in Figure 2, SIS could be electrospun into various cross-linked membranes under such conditions. Figure

2a shows the structure of the membrane composed of various spindle-shaped beads and fibers with varying diameters using a solution concentration of 10 wt%. Most bead-string morphology disappeared (Figure 2b) at a higher solution concentration (13 wt%). As the solution concentration was further increased to 16 wt%, SIS fibers formed smooth surfaces but less cross-linked structures (Figure 2c). The fiber diameters increased as the solution concentration increased for these nonwoven membranes. Similarly, experiments were also performed to investigate the effect of electrospinning voltage and tip-to-collector distance on the morphology of SIS membranes. It was found that optimal conditions were an electrospinning voltage of 20 kV and a tip-to-collector distance of 20 cm, which were subsequently adopted in the following work.

Figure 2: SEM images of SIS membranes electrospun with solution concentration of (a) 10wt%, (b) 13wt%, and (c) 16wt%.

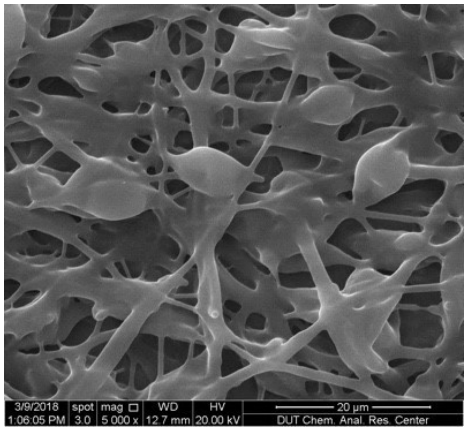

(a) 10 wt%

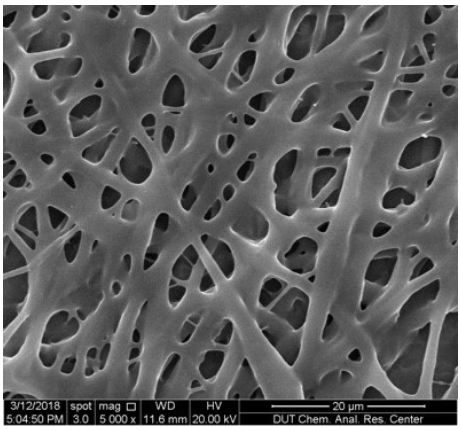

(b) 13 wt%

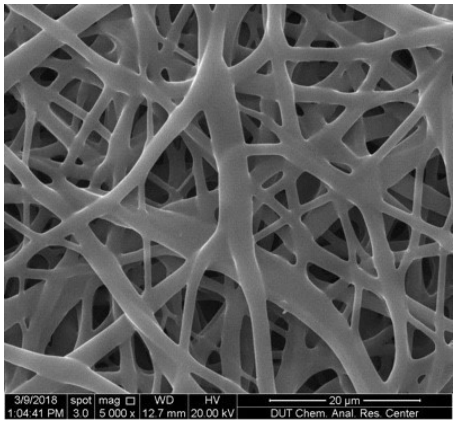

(c) 16 wt%

3.2. Electrospun SIS/C5 PSAs

Although cross-linked SIS membranes could be directly electrospun under optimized conditions, they lacked the adhesion displayed by comparable polymeric nonwoven membranes. To fabricate adhesive materials like spider webs, a tackifier was introduced into the solution used to electrospin SIS/C5 PSAs. SIS/C5 PSAs made by traditional solution casting and melt-processing methods usually require a high C5 content.

Similarly, electrospun SIS/C5 membranes lacked adhesion properties if a small amount of C5 resin was used (< 30 wt%,). Therefore, a series of SIS/C5 PSAs with a thickness of ~ 50 μm were electrospun with variable C5 content based on similar electrospinning conditions except for the SIS/C5 ratio and solution concentration (Table 1). The solvent consisted of DMF, THF and CYH at a weight ratio of 50/25/25. The various SIS/C5 ratios used were 7:3, 6:4, 5:5, 4:6, 3:7, with solution concentrations of 15%, 16%, 17%, 19% and 20%, respectively. They were electrospun with a voltage of 20 kV and relative humidity of 40% at 25±2 °C. The collector rotated at a speed of 400 RPM with a tip-to-collector distance of 20 cm. All samples were collected for 4 hours. The electrospun PSAs were denoted as SCm-n, where m-n represented the SIS/C5 ratio.

Table 1. Electrospinning conditions of SIS/C5 PSAs

Sample	C5 content (%)	Concentration (wt%)
SC7-3	30	15
SC6-4	40	16
SC5-5	50	17
SC4-6	60	19
SC3-7	70	20

Voltage=20 kV, Tip to collector distance = 20 cm

Their adhesion performances were measured in terms of 180° peeling strength and holding power (Table 2). The holding power of all samples was >7 days similar to other melt-processing SIS PSAs (2). Their 180° peeling strength increased with C5 content, as shown in Fig.3. SC7-3 and SC6-4 had lower 180° peeling strength values (0.03 and 0.05 kN/m) due to their low C5 content. As the C5 content increased to 50 wt% in SC5-5, the 180° peeling strength value abruptly increased more than 5 times (0.37 kN/m). This change trend became lesser again as the C5 content was further increased in SC4-6 and SC3-7. In our hands, a minimum C5 content of 50% was required for acceptable adhesive performance of electrospun SIS/C5 PSAs.

Table 2. Performance and structures of electrospun SIS/C5 PSAs

Sample	Porosity (%)	WVP×10^3 ($g/cm^2 \times h$)	Fiber Diameter (μm)	180° Peeling Strength (kN/m)	Holding Power (day)
SC7-3	37.6±0.4	4.1±0.2	1.6±0.2	0.03±0.01	> 7
SC6-4	25.6±0.1	3.7±0.1	1.7±0.1	0.05±0.01	> 7
SC5-5	16.7±0.2	4.1±0.3	1.8±0.1	0.37±0.04	> 7
SC4-6	2.9±0.1	2.0±0.1	2.1±0.2	0.38±0.03	> 7
SC3-7	1.4±0.1	0.9±0.1	2.9±0.3	0.45±0.05	> 7

Figure 3: Plots of porosity and 180° peeling strength versus C5 content in SIS/C5

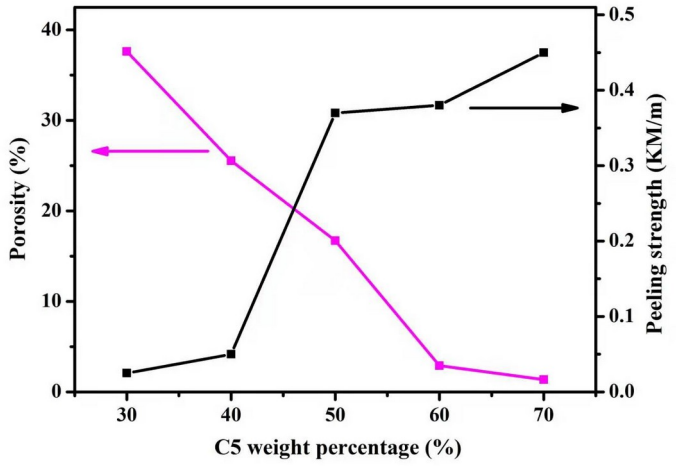

On the other hand, the fiber porosity decreased significantly as the content of C5 increased (Figure 3 and Table 2). SC7-3, SC6-4 and SC5-5 exhibited high porosites of 37.6%, 25.6% and 16.7%, respectively. As the C5 content increased to 60 wt% and 70 wt% in SC4-6 and SC3-7, the porosity significantly decreased (2.9 % and 1.4 %). The change trend of porosity had a close relationship with morphology. SC7-3 had smooth fibers with a diameter of 1.6 μm, which were lightly cross-linked (Figure 4a). As the C5 content increased, the fiber diameter increased but more cross-linked structures were formed in SC6-4 (Figure 4b). This kind of morphology may have contributed to the greater porosity. As the C5 content exceeded 50 wt% of SIS/C5 (Figure 4c and 4d), diameter of the electrospun fibers increased, leading to a decline of the porosity in SIS/C5 membranes. In the case of SC3-7, the porosity was further decreased since the pore structures were nearly closed due to its high load of C5 (Figure 4e). Thus, no attempt was made to electrospin SIS/C5 PSAs with further higher content of C5 resin in the experiments. The formation of pore structures made it possible for the nonwoven SIS/C5 PSAs to have an acceptable water vapor permeability, which was very important for their practical applications. As shown in Table 2, their *WVP* values displayed the same change trend with the increment of C5.

Figure 4 SEM images of membranes: a) SC7-3, b) SC6-4, c) SC5-5, d) SC4-6, e) SC3-7 and f) SC5-5 treated by pressure

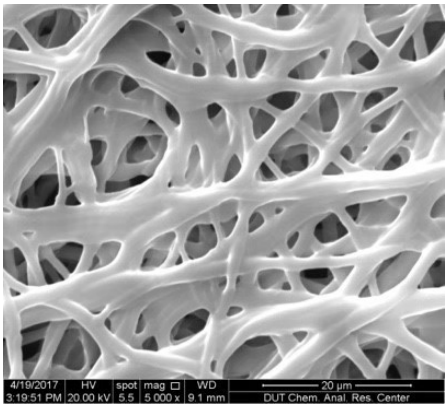

(a) SC7-3

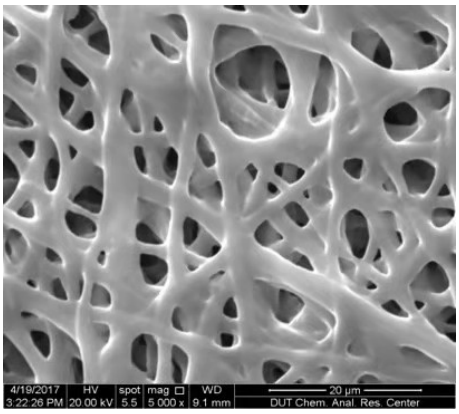

(b) SC6-4

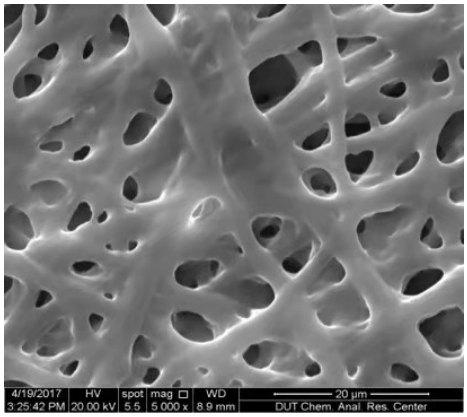

(c) SC5-5

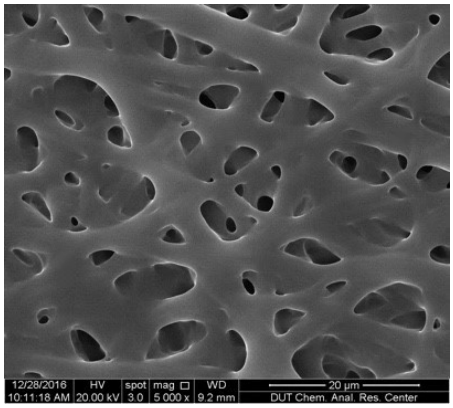

(d) SC4-6

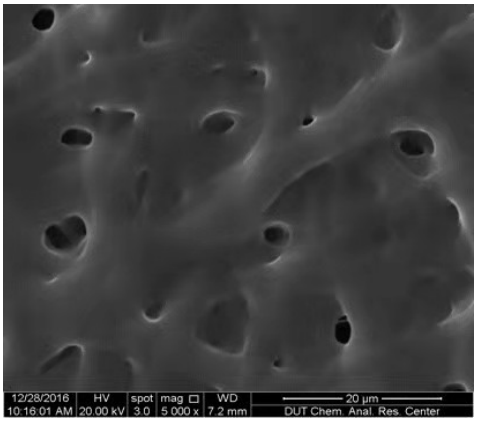

(e) SC3-7

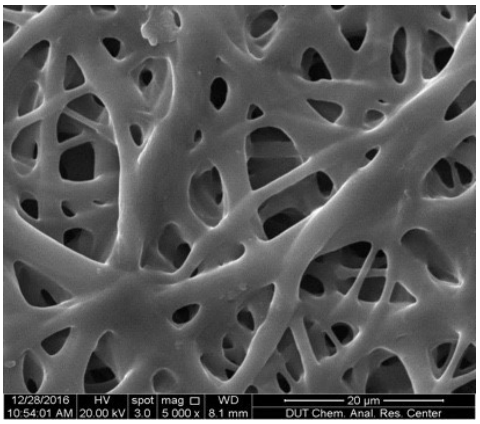

(f) SC5-5, pressure treated

Based on their adhesive performance and porosity/*WVP* results, SC5-5 was chosen as an ideal SIS/C5 PSAs among these nonwoven SIS/C5 membranes. Its dimensional stability was investigated in detail. The SC5-5 strip was pressed onto clean stainless-steel substrates with a 2 kg rubber roller at room temperature. The roller was moved backward and forward three times. After treatment, its morphology was measured by SEM, as shown in Figure 4F. By comparison, no obvious differences were observed for its morphology as shown in Fig.4c and Fig.4f. The ambient pressure did not damage the morphology of SC5-5 due to its good mechanical stability. Meanwhile, its porosity and *WVP* value decreased to a maximum of 14 % under these conditions. To study the effect of thickness, SC5-5-S and SC5-5-L were electrospun using the same electrospinning conditions as SC5-5 except for changing the collection time (2 hours and 8 hours). They were half and twice as thick as SC5-5, respectively. Their structures and properties changed with their thickness (Table 3). Their holding power was > 7 days regardless of the thickness. Although their 180° peeling strength significantly increased with the increment of thickness, it exhibited a steep decline and nearly approached zero as the thickness decreased to 25.2 μm. On the contrary, their porosity and *WVP* value decreased to 1.4 % and 0.91 $g/cm^2 \times h$ with the increment of thickness, respectively. Thus, an optimium thickness was necessary for acceptable adhesive properties as well as air permeability.

Table 3. Performance and structures of SC5-5 with variable thickness

Sample	Thickness (μm)	Porosity (%)	$WVP \times 10^{-3}$ ($g/cm^2 \times h$)	180° Peeling Strength (kN/m)	Holding Power (day)
SC5-5-S	25.2±0.1	37.6±0.2	4.08±0.02	0.03±0.01	> 7
SC5-5	50.1±0.1	16.7±0.1	4.11±0.03	0.37±0.03	> 7
SC5-5-L	100.4±0.3	1.4±0.1	0.91±0.01	0.45±0.05	> 7

4. Conclusions

Nonwoven cross-linked SIS membranes were successfully electrospun without the necessity of explicit solvent removal post treatment, based on which SIS/C5 PSA cross-linked microstructures were fabricated by electrospinning various compositions of SIS/C5 solution. While the SIS membranes did not display any adhesive characteristics like those shown by most other polymeric electrospun membranes, the SIS/C5 PSAs possessed acceptable holding power and variable 180° peeling strength depending on the C5 content. The 180° peeling strength could be significantly increased by increasing the C5 content. A C5 content = 50 wt% was necessary for acceptable adhesive performance. However, above this C5 content, their porosity and *WVP* values decreased, since the diameter of the cross-linked SIS/C5 fibers increased, leading to the disappearance of pore structures. Thus, a SIS/C5 ratio (50:50) was required for optimum adhesive performance, porosity and *WVP*. Adhesive performance, porosity and *WVP* demonstrated a similar change trend with the increase in fiber thickness. Although a greater fiber thickness improved adhesive

properties, excessively large thickness decreased both the porosity and the *WVP*. The electrospun SIS/C5 PSAs were mechanically stable. Thus, changes in processing conditions could produce fibers with tunable properties depending on their desired application.

Acknowledgments
This work was performed at the Dalian University of Technology, Dalian, Liaoning, China. The author appreciates assistance from the analysis center of the Dalian university of technology.

References

1. Gong, M.; Chi, C.; Ye, J.; Liao, M.; Xie, W.; Wu, C.; Shi, R.; Zhang, L. Icariin-loaded electrospun PCL/gelatin nanofiber membrane as potential artificial periosteum. Colloids Surf. B. 2018;170: 201-209. https://doi.org/10.1016/j.colsurfb.2018.06.012

2. Zhang, M.; Ma, W.; Wu, S.; Tang, G.; Cui, J.; Zhang, Q.; Chen, F.; Xiong, R.; Huang, C. Electrospun frogspawn structured membrane for gravity-driven oil-water separation. J. Colloid Interface Sci. 2019;547: 136-144. https://doi.org/10.1016/j.jcis.2019.03.099

3. Liang, Y.; Cheng, S.; Zhao, J.; Zhang, C.; Sun, S.; Zhou, N.; Qiu, Y.; Zhang, X. Heat treatment of electrospun Polyvinylidene fluoride fibrous membrane separators for rechargeable lithium-ion batteries. J. Power Sources, 2013;240: 204-211. https://doi.org/10.1016/j.jpowsour.2013.04.019

4. Wang, W.; Jin, X.; Zhu, Y.; Zhu, C.; Yang, J.; Wang, H.; Lin, T. Effect of vapor-phase glutaraldehyde crosslinking on electrospunstarch fibers. Carbohydr. Polym. 2016;140: 356-361. https://doi.org/10.1016/j.carbpol.2015.12.061

5. Li, L.; Hashaikeh, R.; Arafat, HA. Development of eco-efficient micro-porous membranes via electrospinning and annealing of poly(lacticacid). J. Memb. Sci. 2013;436:57-67. https://doi.org/10.1016/j.memsci.2013.02.037

6. Li, JR.; Fu, R.; Li, L.; Yang, G.; et al. Co-delivery of Dexamethasone and Green Tea Polyphenols Using Electrospun Ultrafine Fibers for Effective Treatment of Keloid. Pharm Res. 2014;31:1632-1643. https://doi.org/10.1007/s11095-013-1266-2

7. Madhaiyan, K.; Sridhar, R.; et al. Vitamin B-12 loaded polycaprolactone nanofibers: A novel transdermal route for the water soluble energy supplement delivery. Int J Pharm. 2013;444:70-76. https://doi.org/10.1016/j.ijpharm.2013.01.040

8. Den, X. Progress on rubber-based pressure-sensitive adhesives. J. Adhesion. 2018;94(2):77-96. https://doi.org/10.1080/00218464.2016.1249573

9. Zhao, Z.; Wang, Z.; Zhang, C.; Li, Z.; Hu, Y. Preparation and characterization of polarity-modulated SIS-based hot melt pressure sensitive adhesives. J Adhes Sci Technol. 2014;28(11):1090-1102. https://doi.org/10.1080/01694243.2014.887255

10. Gennari, C.; Quaronia, G.; Creton, C.; Minghetti, P.; Cilurzo, F. SEBS block copolymers as novel materials to design transdermal patches. Int J Pharm. 2020;575:118975. https://doi.org/10.1016/j.ijpharm.2019.118975